Radial Profiles of the Plasma Electron Characteristics in a 30 kW Arc Jet

Douglas A. Codron*
Universities Space Research Association, NASA Ames Research Center, Moffett Field, CA, 94035

and

Anuscheh Nawaz†
Sierra Lobo, Inc., NASA Ames Research Center, Moffett Field, CA, 94035

The present effort aims to strengthen modeling work conducted at the NASA Ames Research Center by measuring the critical plasma electron characteristics within and slightly outside of an arc jet plasma column. These characteristics are intended to give physical insights while assisting in the formulation of boundary conditions to validate full scale simulations. Single and triple Langmuir probes have been used to achieve estimates of the electron temperature (T_e), electron number density (n_e) and plasma potential (outside of the plasma column) as probing location is varied radially from the flow centerline. Both the electron temperature and electron number density measurements show a large dependence on radial distance from the plasma column centerline with $T_e \approx 3$ - 12 eV and $n_e \approx 10^{12}$ - 10^{14} cm^{-3}.

Nomenclature

A	=	probe surface area (m^2)
b	=	impact factor
c_e	=	electron mean thermal speed (m/s)
c_i	=	ion mean thermal speed (m/s)
e	=	electron charge ($1.602 \cdot 10^{-19}$ C)
I	=	probe current (A)
I_{sat}	=	ion saturation current (A)
J_e	=	electron saturation current density (A/m^2)
J_i	=	ion saturation current density (A/m^2)
k	=	Boltzmann constant ($1.3806 \cdot 10^{-23}$ $m^2 \cdot kg \cdot s^{-2} \cdot K^{-1}$)
m_e	=	electron mass ($9.109 \cdot 10^{-31}$ kg)
m_i	=	ion mass (kg)
n_e	=	electron number density (cm^{-3})
n_{es}	=	electron number density at sheath edge (cm^{-3})
n_{is}	=	ion number density at sheath edge (cm^{-3})
r_p	=	probe radius (m)
T_e	=	electron temperature (eV)
T_i	=	ion temperature (eV)
V_{d2}	=	voltage difference between probes 1 and 2 (V)
V_{d3}	=	applied voltage (V)
ε_0	=	permittivity of free space ($8.854 \cdot 10^{-12}$ $m^{-3} \cdot kg^{-1} \cdot s^4 \cdot A^2$)
λ_D	=	Debye length (m)
λ_{ee}	=	collisional electron-electron mean free path (m)
λ_{ie}	=	collisional ion-electron mean free path (m)
λ_s	=	sheath thickness (m)
ν_{ii}	=	ion collision frequency (s^{-1})

* Mechanical Engineering Intern, Thermo-Physics Facilities Branch, Mail Stop 230-3, Member AIAA.
† Senior Aerospace Engineer, Thermo-Physics Facilities Branch, Mail Stop 229-4, Member AIAA.

I. Introduction

Since 1960, the Arc Jet Complex at NASA Ames Research Center has been a source of long-duration, high-enthalpy flow for materials testing with application to the thermal protection of aerospace vehicle components. From their inception, the facilities have played an integral role supporting many of NASA's space flight programs by simulating the aerodynamic heating environment encountered by spacecraft thermal protection materials and systems upon atmospheric entry.[1] The ability of the Complex's facilities to operate continuously at high power levels (up to 60 MW) while exposing large size samples to simulated aerothermal flight environments has made it unique to the world.

Characterization of the flow environment within these facilities is of great value as the uncertainties arising from measurements of the test conditions and their transfer to computer simulations can result in increased sizing margins to thermal protection systems.[2] Currently, NASA Ames arc jet flow simulations are often based on either a six species (N_2, O_2, NO, N, O and Ar) or a twelve species (N_2, O_2, NO, N, O, N_2^+, O_2^+, NO^+, N^+, O^+, Ar, and e^-) based model which is dependent on solving the conservation equations for hypersonic flows in thermal and chemical nonequilibrium.[3] However, the influence of the free electrons in the energy exchange process is largely unexplored. Therefore, to aid in both the formulation and validation of current models, values of the electron temperature (T_e) and electron number density (n_e) were obtained within the flow of a 30 kW arc jet heater.

This paper presents radial profiles of the electron characteristics obtained in Ames Miniature Arc Jet (mARC), both within and exterior to the plasma column. The mARC facility was constructed and designed with three primary goals:[4] First, to provide experimentally verified boundary conditions to aid in the modeling of arc jet processes, second, to serve as a pre-screening facility for thermal protection system (TPS) materials and TPS sensors in development, and third, to aid in the development of new sensors for plasma characterization. The primary effort of this work is focused on addressing the first and third of these goals via Langmuir probe measurement.

II. Experimental Setup

A. The mARC Facility

The mARC is a subscale arc jet heater in which a continuous electrical discharge between electrodes in the arc chamber heats and expands air at a mass flow rate of approximately 0.45 g/s (in this study) to high temperatures and supersonic velocities. The DC arc jet is composed of a cylindrically symmetric geometry consisting of a water-cooled thoriated tungsten tipped cathode, a water-cooled copper anode, a constrictor channel, and a converging-diverging nozzle. A schematic of the cross section of the mARC can be seen in Figure 1. In operation, a Hypertherm Max 200 30 kW plasma cutting power supply capable of supplying up to 200 A DC establishes a high current regulated arc. The arc is directed from the cathode tip, through a constricted arc column channel, and attaches to the anode. Air is swirled into the arc column through injection ports located behind the cathode. A swirling ring is used to stabilize the arc, constrain the hot gas discharge column to the axis of the vortex, and bring the gas into longer and more effective contact with the arc. The resultant constricted arc heats and largely ionizes the air on the centerline of the constrictor and continues to heat the boundary air through radiation and conduction, resulting in a large radial temperature gradient. It is this large radial temperature gradient which allows the centerline temperature of the heated air to be very high without melting the nozzle. After being directed through the arc column, the hot air is then accelerated out through the convergent-divergent nozzle (1 cm exit diameter) forming a plasma column approximately 1.3 cm in diameter.

The mARC vacuum facility experiments were performed in approximately a 0.61 m in length by 0.3 m diameter cylindrical vacuum chamber (not including feedthrough space) connected to two Leybold Trivac (model # D30A) rotary vane dual stage mechanical vacuum pumps capable of providing base pressures in the 10 mTorr range. Chamber background pressures consistently reached approximately 15 Torr during operation. The mARC was water cooled by a Goulds Pumps e-SV Series vertical multi-stage pump capable of flowing water at 7.885 kg/s. A cooled diffuser was placed at the lower end of the chamber to prevent overheating of the chamber walls due to the high flow temperatures. The layout of the facility can be seen in Figure 2.

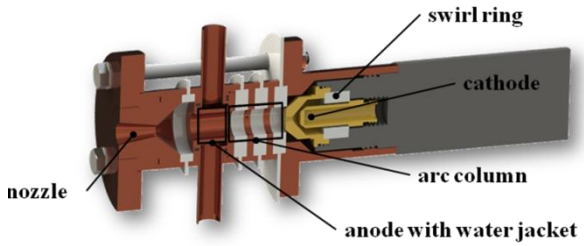

Figure 1: Cross sectional schematic of the mARC[4]

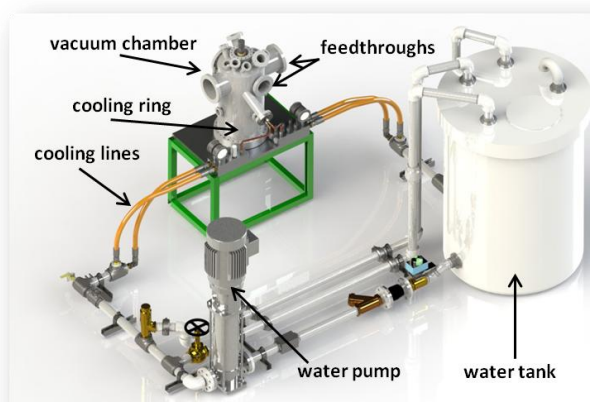

Figure 2: The mARC vacuum facility[4]

B. Langmuir Probes

The plasma electron characteristics were obtained using custom built single and triple Langmuir probes. The tip of the single probe (used for measurements outside of the plasma column) was constructed from a cylindrical tungsten wire 0.61 mm in diameter and approximately 2.5 mm in length, while the triple probe tip consisted of three evenly spaced (~1 mm) tungsten wires each measuring 1.24 mm in diameter and 2.5 mm in length. The larger diameter triple probe tips were used for all plasma column measurements and were necessary to ensure better survivability due to the relatively long (~0.7 sec) periods of time they were exposed to the harsh plasma environment. It has been shown that exposing probe tips for longer periods could lead to an increase of thermionically emitted electrons from its surface and prevent data analysis using assumptions of a nonemitting probe.[5] All probe tips were unshielded and positioned at various distances from the nozzle exit parallel to the flow direction. The single probe bias voltage was swept manually by use of a BK Precision DC regulated power supply (model # 1666) capable of biasing the probe from – 40 to 40 V. For the triple probe, the bias voltage was held constant by three 9 V batteries connected in series. Attached to the chamber and holding both sets of probes was a manually inserted linear actuator providing short residence times as necessary. Probe voltage measurements were recorded with an Agilent Technologies (model # DS06054A) digital oscilloscope supporting a sampling rate of up to 4 GHz. A photograph of the single and triple probes placed outside of the vacuum chamber can be seen in Figures 3a and 3b respectively.

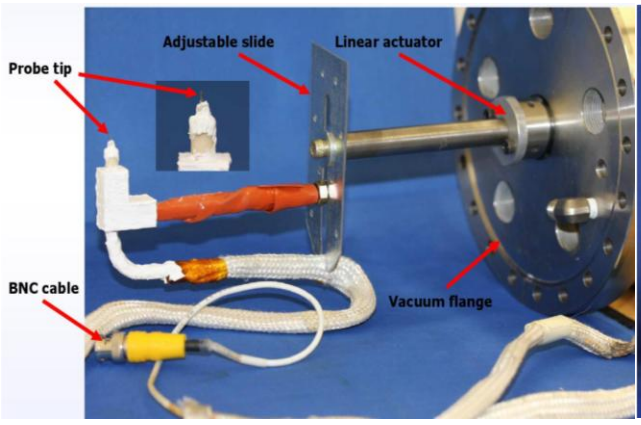

Figure 3a: Photograph of the single Langmuir probe

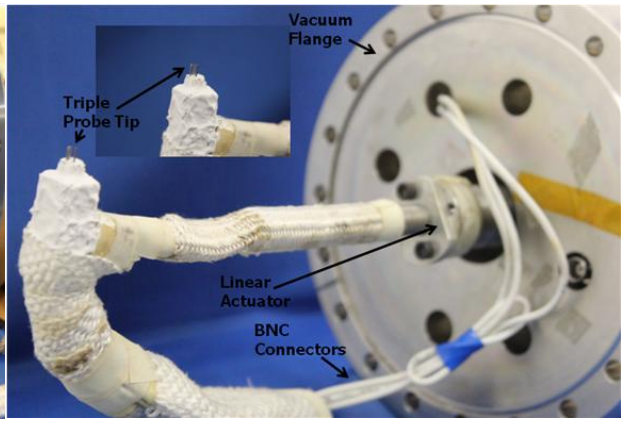

Figure 3b: Photograph of the triple Langmuir probe

Because of the adverse heating effects encountered by the single probe during the long voltage sweeps when inserted into the plasma column, it was decided early on to use a triple probe for all plasma column measurements. A benefit of the triple Langmuir probe is that the sweeping of the bias voltage (as in the case of a single probe) is not required in order to obtain the electron characteristics. By doing so, the analysis is simplified as instantaneous

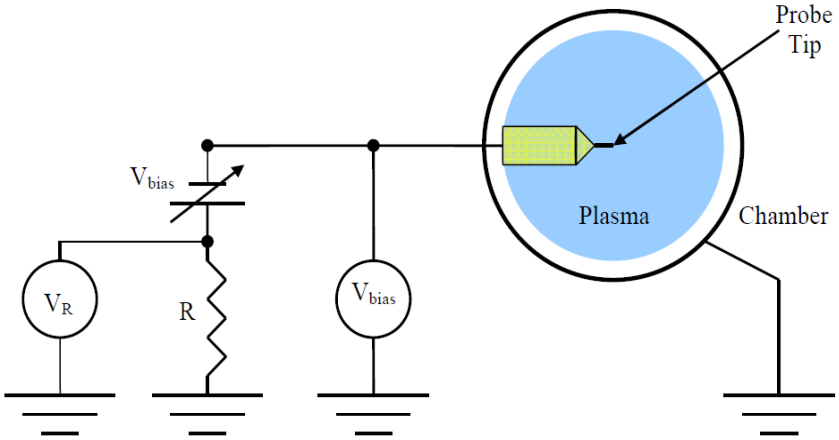

Figure 4: The single Langmuir probe circuit

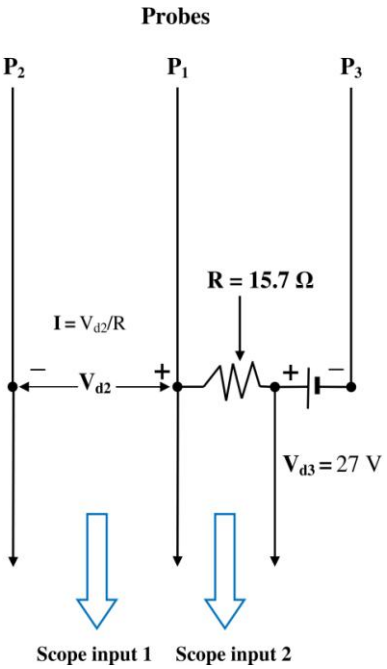

Figure 5: The triple Langmuir probe circuit

values of the electron temperature and electron number density can be obtained.[6] A diagram of the single and triple probe circuits can be seen in Figures 4 and 5 respectively. In the case of the single probe, V_{bias} represents the applied voltage to the probe and V_R represents the voltage measured across the resistor in series with the probe, thus allowing for the measurement of the current (I) through the circuit. Electron temperatures for the single probe were calculated by analyzing the slope of the I-V characteristic in accordance with standard Langmuir probe theory[7] (see results section).

Within the triple probe circuit, a fixed voltage is applied between P_1 and P_3 allowing the current to be measured by noting the voltage drop over a low impedance current carrying resistor. The voltage difference between P_1 and P_2 (which is electrically floating) is also measured allowing for the calculation of the electron temperature and electron density. Several assumptions were made to simplify the analysis for all probe measurements:[8]

1) Because the sheath thickness (λ_s) is much smaller than the probe radius ($\lambda_s << r_p$) a thin sheath analysis was used. Also, the measuring area of the probe was considered to be the entire surface area of the inserted wire. Because the wires have the same dimensions, it was assumed that all probes collect current over the same surface area.

2) The plasma is quasineutral at the sheath edge (i.e., $n_{is} = n_{es}$).

3) A collisionless sheath (λ_s << mean free path) and a sheath thickness smaller than the distance between the probes.

4) The velocities of the electrons and ions at the boundary of the bulk plasma and probe sheath can be approximately represented as Maxwellian distributed.

5) The ion velocity at the plasma boundary is equal or greater than the ion sound speed (i.e., the Bohm sheath criteria holds).

if assumptions 1, 3, and 4 are valid the current flowing into the three probes at any instant may be written as

$$I_1 = AJ_e \exp\left(-\frac{eV_1}{kT_e}\right) - AJ_i(V_1) \tag{1}$$

$$I_2 = AJ_e \exp\left(-\frac{eV_2}{kT_e}\right) - AJ_i(V_2) \tag{2}$$

$$I_3 = AJ_e \exp\left(-\frac{eV_3}{kT_e}\right) - AJ_i(V_3), \tag{3}$$

where J_e is the electron saturation current density, J_i is the ion saturation current density, A is the surface area of the probe, k is Boltzmann's constant, e is the electron charge, and V_1, V_2, and V_3 are the potential difference between the given probe and the space potential. If the relations $J_i(V_1) = J_i(V_2) = J_i(V_3)$ hold, this yields

$$\frac{I_2 - I_1}{I_3 - I_1} = \frac{1 - \exp\left(-\frac{eV_{d2}}{kT_e}\right)}{1 - \exp\left(-\frac{eV_{d3}}{kT_e}\right)}. \tag{4}$$

If $I_2 = 0$ and $I_1 = -I_3$, Eq. (4) reduces to

$$\frac{1 - \exp\left(\frac{-eV_{d2}}{kT_e}\right)}{1 - \exp\left(\frac{-eV_{d3}}{kT_e}\right)} = \frac{1}{2}, \tag{5}$$

allowing for T_e to be determined directly, where V_{d2} and V_{d3} are the voltage difference between P_1 and P_2 and the applied voltage respectively. In the limit $eV_{d3} >> 2kT_e$, Eq.5 simplifies to $kT_e = eV_{d2}/\ln 2$.[9] In addition, if assumptions 2, 4, and 5 are valid[8]

$$n_{is} \cong n_{es} = n_e \exp\left[-\frac{e}{kT_e}\left(\frac{kT_e}{2e}\right)\right] = n_e \exp\left(-\frac{1}{2}\right) \tag{6}$$

and n_e can be directly determined from

$$n_e = \left(\frac{\sqrt{m_i}}{A} I\right) \frac{\exp\left(\frac{1}{2}\right)}{e\sqrt{kT_e}\left[\exp\left(\frac{eV_{d2}}{kT_e}\right) - 1\right]}. \tag{7}$$

It should be noted that even for a thin sheath analysis, it cannot be assumed that there is a constant probe potential with respect to the floating potential (V_f) (as the ion current density is dependent on the electrode potentials). Often, a correction factor β is introduced in order to scale this potential difference. Without the application of the correction factor the electron temperature and electron density can be overestimated at most by 20% and 40% respectively.[10] However, for lower T_e values (~10 eV) the percentage error has been shown to be under 10% with a similar decline in error for the range of n_e values of relevance.[6] Due to the uncertainties in determining a proper correction factor combined with the relatively low electron temperatures characteristic of this study, its influence was ignored.

III. Results and Discussion

A. Single Probe Measurements

Semi-log plotted current-voltage (I-V) profiles were recorded at a location of 75 mm from the nozzle exit, a sample of which can be seen in Figures 6a and 6b. Highlighted are both the electron saturation (green line) and electron transition (red line) regions. Because the ion saturation values are negative, the lowest measured current is subtracted, allowing the electron characteristics to be interpreted on a semi-log scale. The gaps in the curves near zero bias voltages were a product of the manual bias voltage sweep. Because the power supply was incapable of providing a full positive and a full negative sweep, the polarity had to be reversed manually. As a result, it was not uncommon for the negative sweep to begin at values slightly below zero. Since the continuity break did not alter the slope of the electron transition line, there was no discernible impact on the interpretation of the electron measurements.

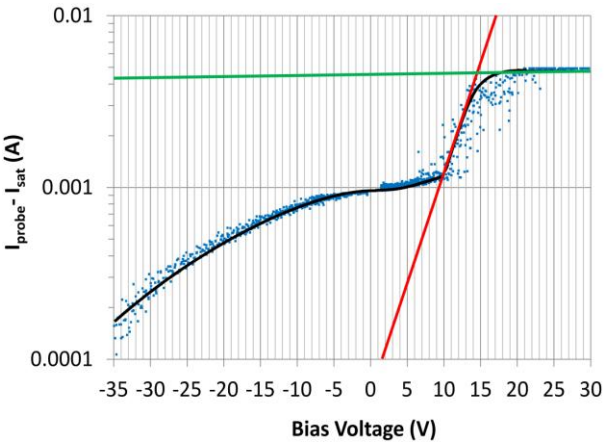

Figure 6a: Single probe I-V curve at 15 mm from the flow centerline and 75 mm from the nozzle exit

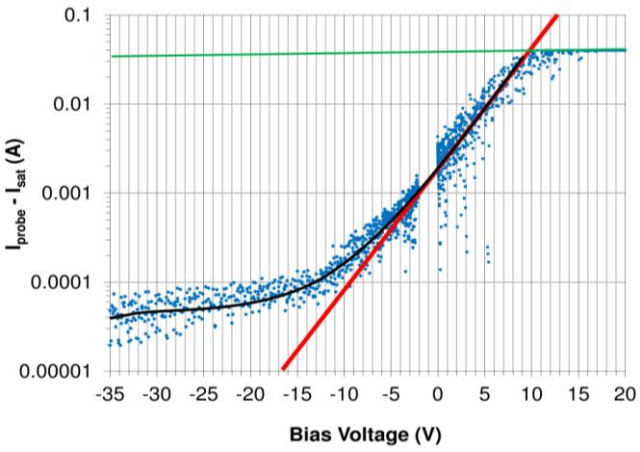

Figure 6b: Single probe I-V curve at 20 mm from the flow centerline and 75 mm from the nozzle exit

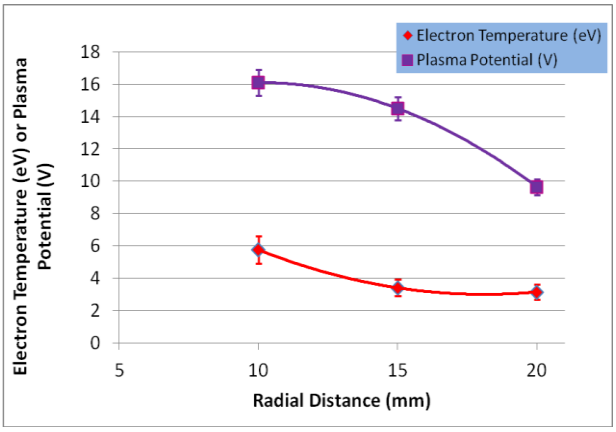

Figure 7: Electron temperature or plasma potential vs. radial distance from the flow centerline at 75 mm from the nozzle exit

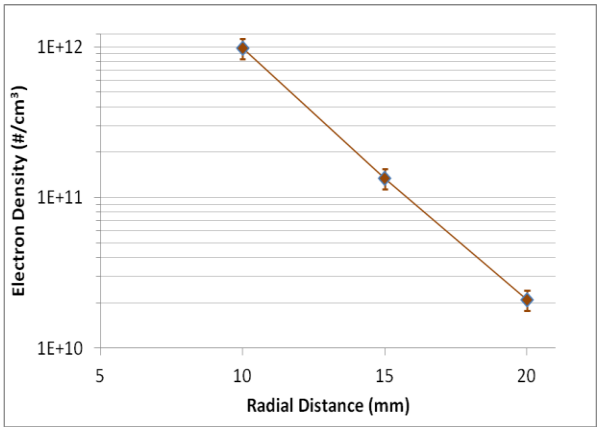

Figure 8: Electron density vs. radial distance from the flow centerline at 75 mm from the nozzle exit

Figure 7 shows the change in both electron temperature and plasma potential with radial distance at 75 mm from the nozzle exit, while Figure 8 shows the changes in electron density for the same conditions. As can be seen from the plots, the ion saturation current is higher for a radial distance of 15 mm from the flow centerline as it is in closer proximity to the plasma column (where there is a larger degree of ionization) than in the 20 mm case. For lengths beyond 20 mm, it was difficult to obtain interpretable ion saturation profiles. Such difficulty may have been due to the tendency of the ions to recombine to form neutrals particles over these larger distances. The electron temperature and electron density both decreased with increasing distance from the plasma column centerline. Single Langmuir probe electron temperatures showed a decrease from 10 mm to 15 mm and began to approach a steadying value at 20 mm. The n_e values were shown to decline exponentially by almost two orders of magnitude over the same radial distance, making it the parameter most heavily influenced. Absolute values of T_e were shown to vary from 3 to 6 eV, while n_e values varied from 1.1×10^{10} cm^{-3} to 10^{12} cm^{-3} over the distance of 1 cm outside of the plasma column, a similar result from a study conducted by Tang et al.[11] The T_e and n_e errors were both due to the interpretation of the slopes of the linear fits of the electron transition regions. Plasma potential error was also a product of the linear fit of the electron transition region as well as the interpretation of where the region intercepted the electron saturation line. It was found that the error (positive and negative) due to the I-V curve fits for all parameters was typically below 20%.

B. Triple Probe Measurements

As mentioned, the difficulty associated with applying a full bias voltage sweep within the short time scales required once the probe was inserted into the plasma column has necessitated the use of a triple Langmuir probe. Unlike single Langmuir probes, triple probes are capable of instantaneously recording a voltage waveform which can be directly converted into electron temperature and density measurements. By doing so, the use of curve fitting was eliminated. Triple probe electron characteristics were measured at 12 mm from the nozzle exit beginning at the plasma column centerline. Following each measurement the probe was moved radially to a distance of 3 mm and then 6 mm from the center. Because the total probe width is on the order of the radial measurement step size, there was a small overlap (~0.5 mm) between regions, making it difficult to identify a precise probing location. Photographs of the position of the probe as it was moved can be seen in Figure 9.

(a) **(b)** **(c)** **(d)**

Figure 9: The triple Langmuir probe and its position in relation to the arc jet plasma column: (a) centered (no flow); (b) centered; (c) 3 mm from the center; (d) 6 mm from the center

As can be seen, substantial wear of the probe ceramic insulation was witnessed after long duration testing (over a few seconds). Therefore, probe exposure was limited to ($t < 0.7$ s) to ensure better survivability and a more precise interpretation of the electron characteristics. Figures 10a – 10d reveal typical triple Langmuir probe electron temperature and electron density traces. The graphs illustrate the substantial high frequency noise which originated from the voltage traces and is attributed more specifically to the tendency of the plasma floating potential to exhibit large oscillations (as recorded by P_2). The noise due to this parameter was shown to lessen with increased discharge current, however it was not able to be eliminated completely. Characteristic of the traces was the tendency for the average values of T_e to reduce fairly quickly ($0.1 < t < 0.3$ s). It has been shown that when the probe is exposed to moderately high electron temperatures (~0.5 eV), the probe surface temperature and the electric field strength may

become sufficiently high enough to promote increased thermionic emission of electrons. In one previous study, electron temperature had been shown to be lowered by as much as 30% when the temperature was increased to only about 2300 K.[12] In this current research, it was not uncommon for the probe to quickly approach the melting point of tungsten (~3700 K), further magnifying this electron temperature reducing effect. To help correct for this tendency, only the stable portions after the initial ramping up period ($0 < t < 0.1$ to 0.2 s) were analyzed. A moving average was applied throughout the entirety of all the traces to help visually smooth the data and to aid in the determination of the region of declining electron temperatures. Once such a region was identified, the range of error was determined from a mean value taken over the analyzed portions of the plots and included data lying within a single standard deviation (both positive and negative). It was found that typically greater than 90% of the recorded data fell within this range.

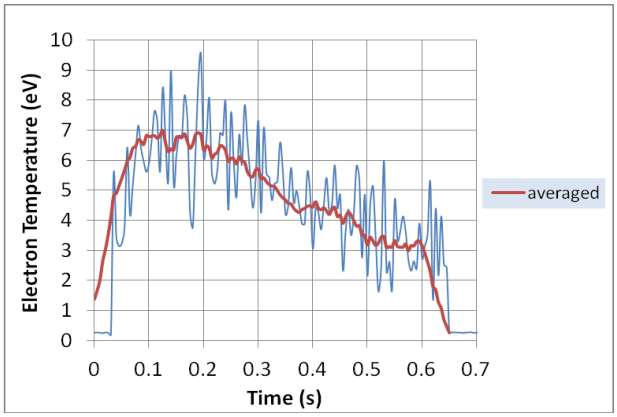

Figure 10a: Electron temperature trace at the plasma column centerline at 80 A

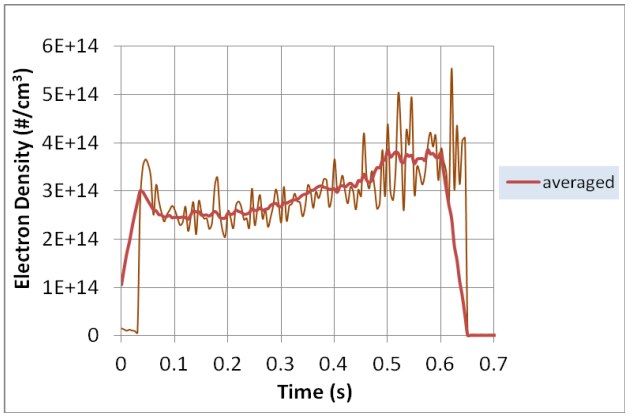

Figure 10b: Electron density trace at the plasma column centerline at 80 A

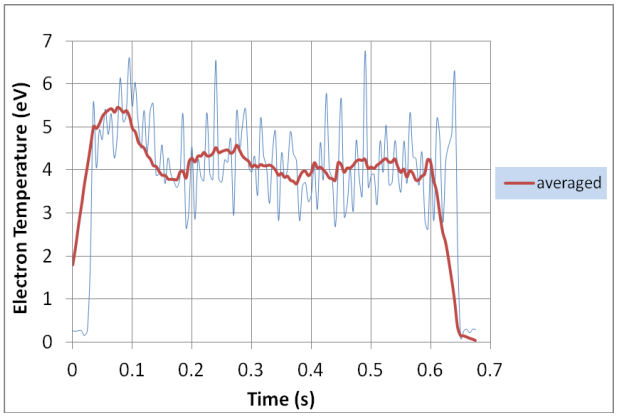

Figure 10c: Electron temperature trace at the plasma column centerline at 100 A

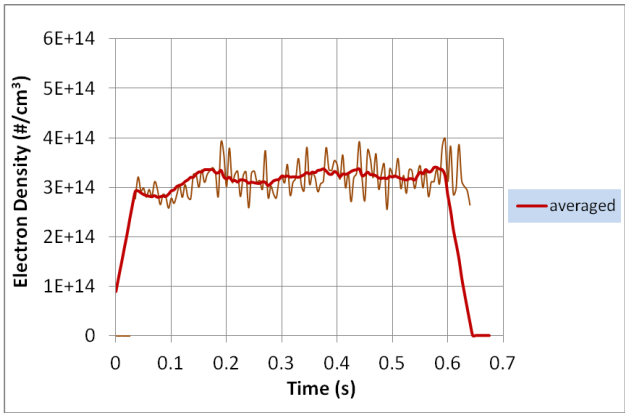

Figure 10d: Electron density trace at the plasma column centerline at 100 A

Figures 11 and 12 show the effects that changes in both radial distance and current have on T_e and n_e respectively. In general, both parameters tended to stay relatively constant over the short radial distance, with T_e values showing a gradual decline and n_e values increasing slightly. Increases in current tended to reduce electron temperature but increase electron density. The lowering of T_e with increased current has been witnessed in similar electrostatic probe studies on arcjet thrusters[13] and magnetoplasmadynamic (MPD) thrusters.[5,14] Increasing the discharge current at these conditions is theorized to increase the rate of collisions with other electrons and heavy particles, thus reducing their initial energy. However, the accelerated rate of electron collisions with neutral particles will increase the ionization fraction, thereby increasing the electron density within the plasma. The larger error bars at lower currents are representative of the increased fluctuating nature of the floating probe voltage traces.

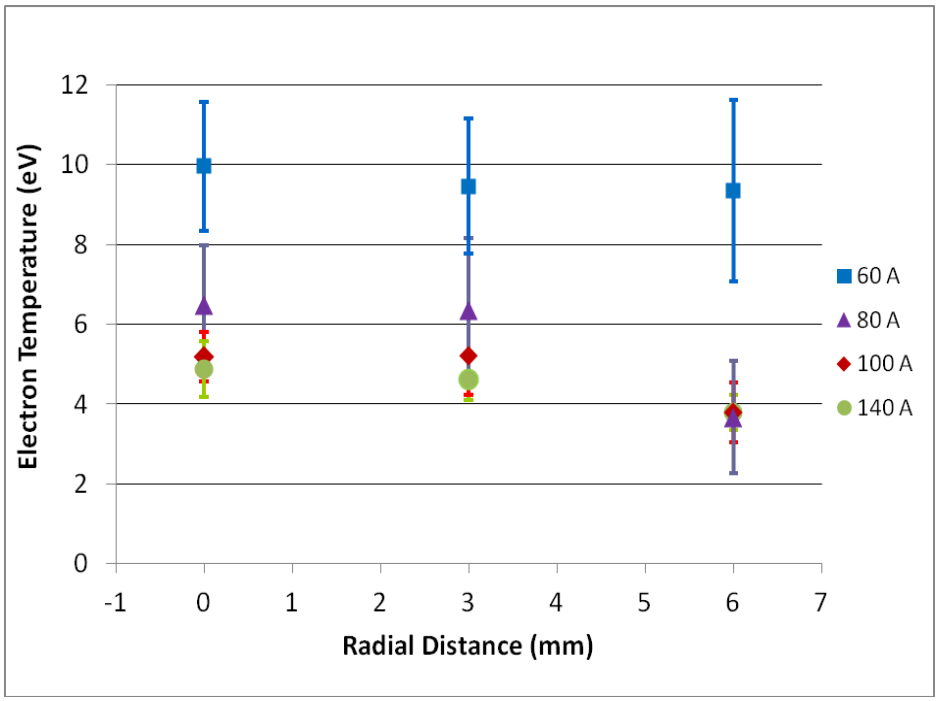

Figure 11: Electron temperature as a function of radial distance from the plasma column centerline at varying discharge currents

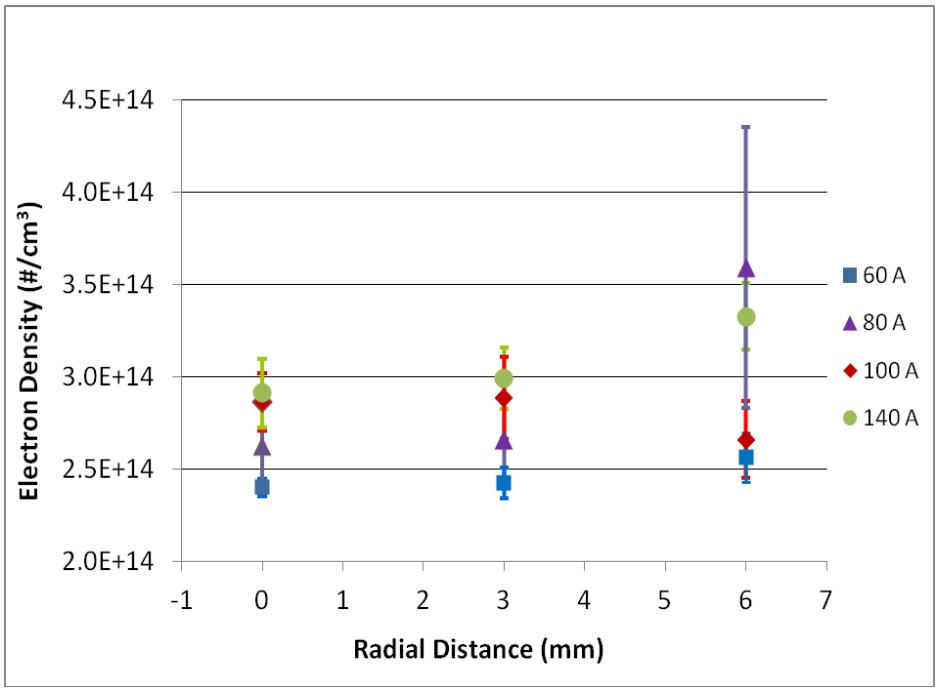

Figure 12: Electron density as a function of radial distance from the plasma column centerline at varying discharge currents

IV. Conclusions

The objective of this study was to measure the electron characteristics in a subscale arc jet heater with the purpose of achieving a better understanding of how changes in probing location and discharge current levels affect electron temperature and electron density measurements. The experimentally verified results are to be applied and transferred to computer simulations aiming to more effectively model the physics of arc jet flows. In general, the electron characteristics of interest showed a weak dependence on radial position with T_e measurements showing a moderate decline with radial distance from the plasma column centerline. Such decline was also witnessed to continue outside of the plasma column. Electron density also exhibited the same small dependence, increasing slightly on average over a distance of 6 mm with a sharp radial decline once outside of the plasma column. For the given conditions, increasing discharge current tended to slightly reduce T_e with the biggest single difference being at the transition from 60 to 80 A. Lastly, electron density tended to increase with increased discharge current with the absolute values of T_e and n_e throughout the entire flow agreeing reasonably well with other studies.

Acknowledgments

The authors would like to thank the tireless efforts of Thanh Ho and Chris Perez for their assistance in data collection and operation of the mARC facility. Also, the contributions and support from David Hash, Tahir Gökçen, Dinesh Prabhu, Brett Cruden, Joe Hartman, Jose Santos, and George Raiche are gratefully acknowledged. We also would like to thank the NASA Strategic Capabilities Assets Program (SCAP) for supporting arc jet instrumentation development.

References

[1]Balter-Peterson, Aliza, et al. "Arc jet testing in NASA Ames Research Center thermophysics facilities." *AIAA Materials Specialist Conference-Coating Technology for Aerospace Systems*. Vol. 1. 1992.

[2]Grinstead, Jay H., Driver, David M., and Raiche, George A.. "Radial profiles of arcjet flow properties measured with laser-induced fluorescence of atomic nitrogen." *Instrumentation in Aerospace Simulation Facilities, 2003. ICIASF'03. 20th International Congress on*. IEEE, 2003.

[3]Fletcher, Douglas G. "Measurement requirements for improved modeling of arcjet facility flows." *Measurement Techniques for High Enthalpy and Plasma Flows*, *NATO Research and Technology Organization Proceedings RTO-EN-8*, Neuilly-Sur-Seine Cedex, France, (2000): 3A-1-3A-27.

[4]Nawaz, Anuscheh, Philippidis, Daniel, and Ho, Thanh. "Setup and characterization of the 30 kW arc jet facility mARC." *44th AIAA Thermophysics Conference*, San Diego, CA., 2013.

[5]Codron, Douglas, et al. "Solid thoriated tungsten cathode arc discharges for electrically propelled spacecraft." *IEEE Transactions on Plasma Science* 40.7 (2012): 1926-1932.

[6]Chen, Sin‐Li, and T. Sekiguchi. "Instantaneous direct‐display system of plasma parameters by means of triple probe." *Journal of Applied Physics* 36.8 (1965): 2363-2375.

[7]Chen, F.F. "Electric Probes" *Plasma Diagnostic Technique*, ed. R. H Huddlestone and S.L. Leonard, New York: Academic, (1965): 113-200.

[8]Eckman, Robert Francis. "Langmuir probe measurements in the plume of a pulsed plasma thruster." *Thesis*. Worcester Polytechnic Institute-NASA, 1999.

[9]Naz, Muhammad Yasin, et al. "Double and triple Langmuir probes measurements in inductively coupled nitrogen plasma." *Progress In Electromagnetics Research* 114 (2011): 113-128.

[10]Auweter-Kurtz, Monika, Feigl, Markus, and Winter, Michael. "Diagnostic tools for plasma wind tunnels and reentry vehicles at the IRS." *Paper presented on the RTO AVT Course on Measurement Techniques for High Enthalpy and Plasma Flows*, Rhode-Saint-Genèse, Belgium, published in RTO EN-8, Oct. 1999.

[11]Tang, J. T., Luhmann Jr., N. C., Turechek, J, and Jassby, D. L.. "A steady-state high-density magnetized arcjet plasma." *Journal of Applied Physics*, 46.8 (1975): 3376-3380.

[12]Chen, Che Jen. "Temperature effect on Langmuir Probe Measurements." *Journal of Applied Physics*, 35.4 (1964): 1130-1133.

[13]Bufton, Scott A., Burton, Rodney, L.. "Velocity and temperature measurements in a low-power hydrazine arcjet." *AIAA Journal of Propulsion and Power* 13.6 (1997): 768-774.

[14]Downey, Ryan T., et al. "Single-channel hollow cathodes in 5-20 eV Argon Discharge for Spacecraft Thruster Applications." *IEEE Transactions on Plasma Science*, 39.4 (2011): 1075-1081.

Appendix

To ensure a collisionless sheath, the distance between the mean free paths of the ion-ion (λ_{ii}) and ion-electron (λ_{ie}) collisions were estimated from: [8]

$$\lambda_{ii} = \frac{c_i}{\nu_{ii}} \tag{8}$$

and

$$\lambda_{ie} = \frac{c_e}{\nu_{ii}\sqrt{\frac{m_i}{2m_e}}\left(\frac{T_i}{T_e}\right)^{\frac{3}{2}}}, \tag{9}$$

where the mean thermal speed for the species P (= i,e) is represented by

$$c_P = \sqrt{\frac{8kT_P}{\pi m_P}}. \tag{10}$$

The ion collision frequency is given by

$$\nu_{ii} = n_i c_{ii} 6\pi b^2 \ln\left(\frac{\lambda_D}{b}\right), \tag{11}$$

where

$$b = \frac{e^2}{4\pi\varepsilon_0 m_i {c_{ii}}^2} \tag{12}$$

is the impact parameter. Finally, in order to estimate the sheath thickness, the Debye length was given by

$$\lambda_D = \sqrt{\frac{\varepsilon_0 k T_e}{e^2 n_e}} \ , \tag{13}$$

where ε_0 is the permittivity of free space. The sheath thickness is expected to be on the order of a few Debye lengths. For the total range of T_e and n_e values in this work, the Debye length was found to be between 0.002-0.0006 mm – significantly less than the probe radius. The mean free path of the electrons were estimated to be between 1 to 100 mm, validating the assumption of collisionless sheaths.